DALTON
FULL PAPER

Copper(II) complexes of hydroquinone-containing Schiff bases. Towards a structural model for copper amine oxidases

Peiyi Li,[a] Nayan K. Solanki,[a] Helmut Ehrenberg,[ab] Neil Feeder,[a] John E. Davies,[a] Jeremy M. Rawson[a] and Malcolm A. Halcrow*[c]

[a] *Department of Chemistry, University of Cambridge, Lensfield Road, Cambridge, UK CB2 1EW*
[b] *Interdisciplinary Research Centre in Superconductivity, University of Cambridge, Madingley Road, Cambridge, UK CB3 0HE*
[c] *School of Chemistry, University of Leeds, Woodhouse Lane, Leeds, UK LS2 9JT. E-mail: M.A.Halcrow@chem.leeds.ac.uk*

Received 17th February 2000, Accepted 31st March 2000
Published on the Web 17th April 2000

Complexation of the preformed ligand 2,5-dihydroxy-*N*-{pyridin-2-ylmethyl}-benzylideneamine (HL^1) with hydrated $Cu(BF_4)_2$ afforded $[\{Cu(\mu\text{-}L^1)\}_2][BF_4]_2$ **1**. The crystal structure of **1**·$MeNO_2$ shows a dimer of near-planar copper(II) ions, with a bridging apical BF_4^- anion. Variable temperature susceptibility measurements showed the copper(II) ions in **1** to be moderately antiferromagnetically coupled. The complexes $[CuL^2]X$ ($X^- = ClO_4^-$ **2**, NO_3^- **3**, Cl^- **4** or NCS^- **5**) and $[CuL^3]ClO_4$ (**6**; HL^2 = *N*-{pyridin-2-ylmethyl}-*N*′-{2,5-dihydroxybenzylidene}-1,2-diaminoethane, HL^3 = *N*-{pyridin-2-ylmethyl}-*N*′-{2,4,5-trihydroxybenzylidene}-1,2-diaminoethane) have been prepared by template condensation of *N*-(pyridin-2-ylmethyl)-1,2-diaminoethane with the appropriate benzaldehyde derivative and copper salt. The single crystal structure of **2** shows a near-planar four-co-ordinate copper(II) centre, with a non-co-ordinated ClO_4^- anion. The chelate ligand backbone is disordered over two orientations, which correspond to different patterns of intermolecular hydrogen bonding in the lattice. UV/vis and EPR data in dmf solution suggest that **2**–**6** all undergo solvolysis to form an identical $[CuL(dmf)_x]^+$ ($x = 0$–2) species in solution. Cyclic voltammograms of HL^1 and **1**–**6** are complex, and demonstrate rapid acid-catalysed decomposition of the benzoquinonecarbaldimine ligand oxidation products.

Introduction

Copper-containing amine oxidases (CAOs) catalyse the aerobic oxidation of primary amines, eqn. (1), and are ubiquitous in

$$RCH_2NH_2 + O_2 + H_2O \longrightarrow RCHO + NH_3 + H_2O_2 \quad (1)$$

nature, having been isolated from organisms as diverse as bacteria, yeast, plants and mammals, including humans.[1] From EXAFS,[2] EPR,[3] NMR,[4] mutagenesis[5] and crystallographic[6] data it is known that CAOs contain a mononuclear copper centre with a $[Cu(His)_3(OH_2)_n]^{+/2+}$ ($n = 0$ or 2) co-ordination sphere, together with the cofactor topaquinone (TPQ, 2,4,5-trihydroxyphenylalaninequinone).[7] The TPQ residue is very mobile within the active site, and has been observed crystallographically to be either co-ordinated to the copper ion (Fig. 1a) or to lie 3–5 Å from it (Fig. 1b). The latter structural form represents the resting state of a catalytically active CAO molecule.

The amine oxidation chemistry is performed by the TPQ residue, which is concomitantly reduced to an amino-TOPA derivative (TOPA = 2,4,5-trihydroxyphenylaniline) by a well characterised mechanism.[8] The role of the copper ion in reoxidising the reduced co-factor back to TPQ is less clear.[9] There is crystallographic evidence that O_2 binds close to the copper ion, although the observed $Cu\cdots O_2$ distance of 2.9 Å is too long to be called a 'proper' co-ordinative bond.[10] A catalytically competent temperature- or cyanide-dependent valence tautomerism equilibrium has also been characterised in substrate-reduced CAO (eqn. (2); TPSQ = 2,4,5-trihydroxyphenylalaninesemiquinone),[11] and may represent a pathway for TOPA→Cu electron transfer during catalysis. However, recent kinetic data have thrown the role of copper as an electron acceptor in the CAO oxidative half-reaction into some doubt.[9] Little model chemistry that could shed light on these questions has been published to date.[12–14]

$$Cu^{II}/TOPA \rightleftharpoons Cu^{I}/TPSQ \quad (2)$$

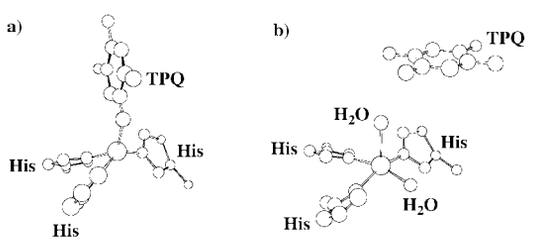

Fig. 1 Views of the TPQ-on (a) and TPQ-off (b) forms of the active site of copper amine oxidase. For simplicity, only the methylene carbon atom of the cofactor is shown.

We have recently described a synthetic, spectroscopic and electrochemical study of a series of salen-analogue Schiff base complexes derived from 2,5-dihydroxybenzaldehyde.[15] This study showed that Schiff base formation was potentially a facile route to the incorporation of a hydroquinone moiety into a polydentate ligand. As a complement to our continuing work on galactose oxidase model chemistry,[16] we have, therefore, embarked on a program to prepare new Cu^{II}/quinone or Cu^{II}/hydroquinone complexes to attempt to address the role of copper in CAO catalysis. Our target compounds for this work are mononuclear four-co-ordinate copper(II) complexes bearing one hydroquinonate moiety, which have potential for copper- and ligand-centred redox chemistry that mimics that undergone

This journal is © The Royal Society of Chemistry 2000

by CAO. This paper describes our initial efforts towards this end.

Results and discussion

Complexes of tridentate Schiff base ligands

Reaction of 2-(2-aminoethyl)pyridine (Scheme 1) with 1 molar equivalent of 2,5-dihydroxybenzaldehyde in refluxing MeOH afforded a yellow solution. Evaporation of this solution to dryness yielded a deep yellow oil, from which a mustard-coloured solid HL^1 could be isolated in near-quantitive yield following trituration with the minimum volume of Et_2O. Complexation of hydrated $Cu(BF_4)_2$ with 1 equivalent of HL^1 in $MeNO_2$ afforded a deep brown solution, which deposited an oily solid following concentration and layering with Et_2O; recrystallisation of this crude product from $MeNO_2$–Et_2O afforded a dark brown crystalline material. Upon drying, this solid analysed reproducibly as $[CuL^1]BF_4 \cdot \frac{1}{2}H_2O$. However, FAB mass spectrometry showed a strong peak at $m/z = 607$, assignable to the fragment $[^{63}Cu_2(L^1)_2 - H]^+$. Hence, this complex was assigned a dimeric formulation $[\{Cu(\mu\text{-}L^1)\}_2][BF_4]_2$ **1**, which was subsequently confirmed by crystallography (see below).

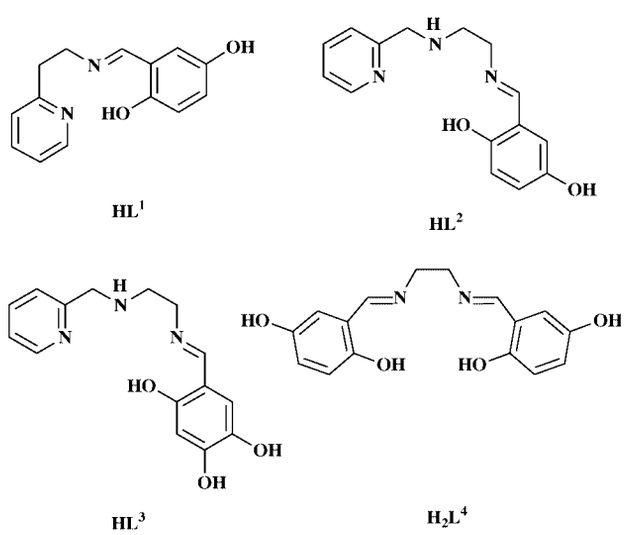

Scheme 1 Ligands referred to in this study.

In addition to the above reaction, a large number of complexations were attempted of other copper(II) salts by HL^1, and by other tridentate ligands derived by condensation of 2,5-dihydroxybenzaldehyde or 2,4,5-trihydroxybenzaldehyde with 2-aminomethylpyridine, *N*,*N*-dimethyl-1,2-diaminoethane or histamine (imidazole-4-ethanamine). In all cases, brown oils were obtained from the reaction mixtures that could not be further purified. From some reactions carried out in MeCN, colourless crystals of $[Cu(NCMe)_4]BF_4$ could be isolated from the brown oily residue. Attempted template syntheses of complexes using 2,5-dihydroxybenzaldehyde, the appropriate chelating diamine and hydrated $Cu(BF_4)_2$, $Cu(ClO_4)_2$ or $CuCl_2$ were similarly unsuccessful. We suggest that the intractability of this system originates from partial reduction of the copper content of the reaction mixtures to Cu^I (see above), the reducing agent probably being 2,5-dihydroxybenzaldehyde.

Single crystals of formula $[\{Cu(\mu\text{-}L^1)\}_2][BF_4]_2 \cdot MeNO_2$ (**1**·$MeNO_2$) were grown from $MeNO_2$–Et_2O by vapour diffusion. The structure contains one dimeric molecule lying on a general position (Fig. 2, Table 1). The two copper ions adopt tetragonal geometries, with typical Cu–N and Cu–O distances[17] and an approximately planar arrangement of basal donors, the *trans*-N–Cu–O angles within the basal planes of the two ions being 159.5(3)–166.7(3)° (Table 1). The basal $[N_2Cu(\mu\text{-}O)_2CuN_2]$ unit of the complex is not planar, the least

Table 1 Selected bond lengths (Å) and angles (°) for $[\{Cu(\mu\text{-}L^1)\}_2][BF_4]_2 \cdot MeNO_2$ (**1**·$MeNO_2$). Primed atoms are related to their unprimed equivalents by the relation $1 - x, 1 - y, 2 - z$

Cu(1)···Cu(2)	2.9852(16)	Cu(2)–O(19)	1.976(5)
Cu(1)–N(3)	1.987(7)	Cu(2)–N(21)	1.968(7)
Cu(1)–N(11)	1.949(7)	Cu(2)–N(29)	1.937(7)
Cu(1)–O(19)	1.933(5)	Cu(2)–O(37)	1.935(5)
Cu(1)–O(37)	1.970(5)	Cu(2)···O(38′)	2.736(7)
Cu(1)···F(42)	2.558(5)	Cu(2)···F(40)	2.869(7)
N(3)–Cu(1)–N(11)	95.8(3)	O(19)–Cu(2)–F(40)	105.6(2)
N(3)–Cu(1)–O(19)	163.3(3)	N(21)–Cu(2)–N(29)	95.7(3)
N(3)–Cu(1)–O(37)	96.1(3)	N(21)–Cu(2)–O(37)	159.5(3)
N(3)–Cu(1)–F(42)	83.2(2)	N(21)–Cu(2)–O(38′)	104.0(2)
N(11)–Cu(1)–O(19)	93.7(3)	N(21)–Cu(2)–F(40)	79.5(2)
N(11)–Cu(1)–O(37)	166.7(3)	N(29)–Cu(2)–O(37)	93.4(3)
N(11)–Cu(1)–F(42)	95.8(2	N(29)–Cu(2)–O(38′)	85.0(2)
O(19)–Cu(1)–O(37)	76.3(2)	N(29)–Cu(2)–F(40)	82.0(2)
O(19)–Cu(1)–F(42)	82.2(2)	O(37)–Cu(2)–O(38′)	95.1(2)
O(37)–Cu(1)–F(42)	91.5(2)	O(37)–Cu(2)–F(40)	83.6(2)
O(19)–Cu(2)–N(21)	97.3(3)	O(38′)–Cu(2)–F(40)	166.82(17)
O(19)–Cu(2)–N(29)	165.9(3)	Cu(1)–O(19)–Cu(2)	99.6(2)
O(19)–Cu(2)–O(37)	76.1(2)	Cu(1)–O(37)–Cu(2)	99.7(2)
O(19)–Cu(2)–O(38′)	86.7(2)		

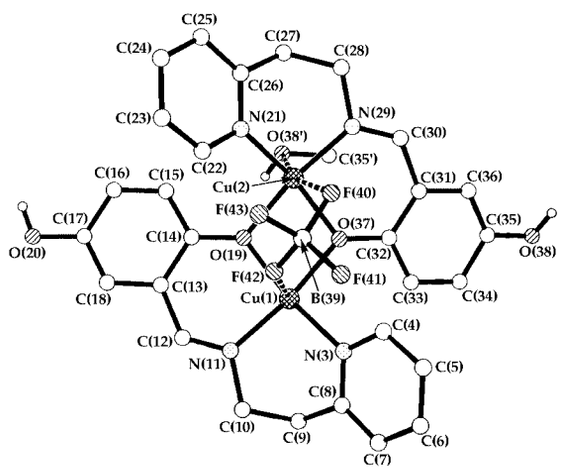

Fig. 2 View of the complex cation in the structure of $[\{Cu(\mu\text{-}L^1)\}_2][BF_4]_2 \cdot MeNO_2$, showing the atom numbering scheme employed. Primed atoms are related to unprimed atoms by the relation $1 - x, 1 - y, 2 - z$. For clarity, all C-bound H atoms have been omitted.

squares basal planes of the two Cu ions, [Cu(1), N(3), N(11), O(19), O(37)] and [Cu(2), O(19), N(21), N(29), O(37)], forming a dihedral angle of 40.2(3)°. The Cu(1)···Cu(2) distance is 2.985(2) Å, while the bridging Cu–O–Cu angles are Cu(1)–O(19)–Cu(2) 99.6(2) and Cu(1)–O(37)–Cu(2) 99.7(2)°. Although there are some deviations from trigonality, the sums of angles at O(19) and O(37) are 359.1(7) and 360.0(7)° respectively, showing that both bridging O atoms are almost perfectly planar.

In addition to the bridging phenoxide donors the copper ions are bridged by weak axial interactions to one BF_4^- anion, with Cu(1)···F(42) 2.558(5) and Cu(2)···F(40) 2.869(7) Å. There is also a weak intermolecular axial interaction to Cu(2) from a 5-hydroxyl group on one $[L^1]^-$ ligand of a neighbouring molecule (related by $1 - x, 1 - y, 2 - z$), with Cu(2)···O(38′) 2.736(7) Å. Hence, Cu(1) adopts a square pyramidal geometry, while the geometry at Cu(2) is better described as a distorted octahedron (Fig. 2). The hydroxyl group O(20)–H(20) is hydrogen bonded to the second (disordered) BF_4^- anion, with the following metric parameters: O(20)···F(45″) 2.961(10), O(20)–H(20)···F(45″) 135°; O(20)···F(48A″) 2.847(14) Å, O(20)–H(20)···F(48A″) 153°; and O(20)···F(48B″) 2.739(18) Å, O(20)–H(20)···F(48B″) 163°. For these interactions, primed atoms are related to unprimed atoms by $2 - x, -y, 1 - z$, while F(48A) and F(48)B are different disorder orientations of the

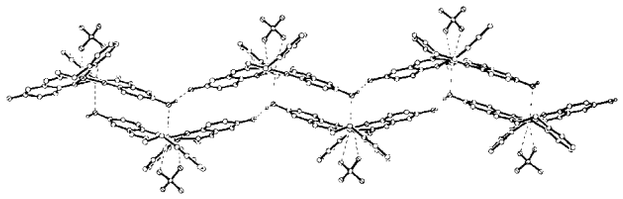

Fig. 3 Partial packing diagram of the structure of $[\{Cu(\mu\text{-}L^1)\}]_2[BF_4]_2\cdot MeNO_2$ (**1**·$MeNO_2$), showing the 'dimer of chains' packing motif. For clarity, all C-bound H atoms, and the non-co-ordinated anion and solvent molecule, have been omitted.

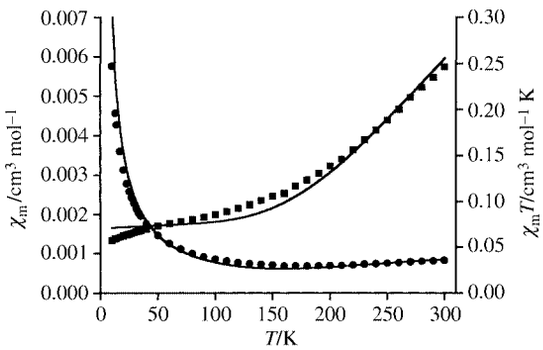

Fig. 4 Plots of χ_m *vs.* T (circles) and $\chi_m T$ *vs.* T (squares) for complex **1**. The solid lines represent best fits of the data by the Bleaney–Bowers equation; see text for details and fitting parameters.

same F atom (see Experimental section). There are no close contacts between the complex cation and the CH_3NO_2 solvent molecule.

In addition to the above intermolecular interaction, the complex molecules are linked into chains by intermolecular hydrogen bonds between 5-hydroxyl groups of molecules related by $1 + x$, $-1 + y$, $-1 + z$, the O(20)···O(38‴) distance being 2.731(9) Å and O(20)···H(38‴)–O(38‴) 172°. There are also intermolecular π–π-stacking interactions between phenol rings of the complexes: C(13)–C(18) and C(13″)–C(18″) [$2 - x$, $-y$, $1 - z$], which are separated by 3.3 Å and whose centroids are offset by 1.3 Å; and C(31)–C(36) and C(31′)–C(36′) [$1 - x$, $1 - y$, $2 - z$], which are separated by 3.2 Å and are offset by 1.6 Å. In both cases the stacked aromatic rings are strictly coplanar by symmetry. The effects of these interactions are to link the complex cations into 'pairs of chains' in the crystal lattice (Fig. 3), the molecules associating into 1-dimensional chains by hydrogen bonding, and each chain within the dimer being linked by weak axial Cu···O and π–π-stacking interactions. Adjacent 'pairs of chains' in the lattice interact by van der Waals contacts only.

Variable susceptibility data on dried, powdered crystals of complex **1** were collected between 300 and 10 K (Fig. 4). The $\chi_m T$ *vs.* T curve is typical of a strongly antiferromagnetically coupled system, as expected for a diphenoxo-bridged Cu^{II}_2 dimer.[18] The data were analysed using the Bleaney–Bowers equation, with corrections for a mononuclear impurity and temperature-independent paramagnetism, according to the $H = -2J(S_1\cdot S_2)$ spin Hamiltonian, eqn. (3).[19] A reasonable fit of

$$\chi_m = \frac{2Ng^2\beta^2}{kT}\left[3 + \exp\left(\frac{-2J}{kT}\right)\right]^{-1}(1-\rho) + \frac{Ng^2\beta^2}{2kT}\rho + 2N_a \quad (3)$$

$\chi_m T$ was obtained for $J = -285$ cm^{-1} and $\rho = 0.09$ (Fig. 4). During the refinements g converged consistently to values of 2.0–2.1, and so was fixed at 2.1 for the final fit; N_a was also fixed at 60×10^{-6} cm^3 mol^{-1}. This J value is somewhat lower than would be expected from the correlation of J with the Cu–O–Cu bridging bond angle ('a') for macrocyclic $[Cu_2(\mu\text{-phenoxide})_2]^{2+}$ compounds published by Thompson and co-workers, which predicts $J \approx -360$ cm^{-1} for $a = 99.7°$.[18] This may reflect the non-macrocyclic nature of **1**, which removes Thompson's proposed additional antiferromagnetic superexchange pathway for macrocyclic Schiff base complexes *via* a conjugated 2,6-bis-(carbaldimino)phenoxy fragment.[18] Alternatively, the bent, rather than planar, Cu_2O_2 bridge shown by **1** (see above) might also be expected to make J less negative.[20] Incorporation of a Weiss constant into the equation to allow for interdimer interactions did not noticeably improve the refinement. This is consistent with the crystal structure of **1**·CH_3NO_2, in which the shortest potential intermolecular superexchange pathway is *via* the apical Cu(1)···O(38′) interaction (Figs. 2 and 3). This is 7 bonds in length, and does not involve the d_{xy} magnetic orbital at copper. Intermolecular superexchange would therefore be expected to be negligible.

In the powder complex **1** is EPR-silent at 293 and 77 K. The X-band EPR spectrum in MeCN at 77 K exhibits only a very weak isotropic signal at $\langle g \rangle = 2.08$, with no hyperfine coupling being apparent. No half-field absorption that would be indicative of population of a triplet spin state[21] was observed. These data imply that the major species present in MeCN solutions of **1** is the intact antiferromagnetically coupled $[\{Cu(\mu\text{-}L^1)\}_2]^{2+}$ dication, with only a small amount of solvolysis product $[Cu(L^1)(MeCN)_x]BF_4$ ($x = 1$–3) being formed. The visible spectrum of **1** in MeCN is dominated by O→Cu LMCT absorptions,[22] which appear as shoulders at $\lambda_{max} = 390$ and 475 nm. The d–d bands from the copper(II) ions[23] also occur as shoulders, near 610 and 900 nm.

Complexes of tetradentate Schiff base ligands

Since the copper(II) complex chemistry of $[L^1]^-$ and its tridentate analogues is barely tractable and complicated by dimerisation processes, we decided to examine the co-ordination chemistry of related tetradentate imine ligands derived from *N*-(pyridin-2-ylmethyl)-1,2-diaminoethane as a means of obtaining mononuclear Cu^{II}/hydroquinone complexes. Surprisingly, there is only one previous report of a Schiff base derived from this diamine,[24] although the closely related complex [CuCl(paip)] (Hpaip = *N*-{2-hydroxybenzaldimino}-*N*′-{pyridin-2-ylmethyl}-1,3-diaminopropane) did appear during the course of this work.[25] Attempts to prepare HL^2 and HL^3 by reaction of *N*-(pyridin-2-ylmethyl)-1,2-diaminoethane with an equimolar amount of the appropriate benzaldehyde derivative in refluxing MeOH or MeCN afforded in all cases crude residues following removal of the solvent, which contained predominantly the imidazoline derivatives $NC_5H_4CH_2\overline{NC_2H_4NHC}HR$ (R = $C_6H_3\{OH\}_2$-2,5-X-4; X = H or OH) by ^{1}H NMR. Therefore, template syntheses of complexes containing the $[CuL]^+$ ($L^- = [L^2]^-$ or $[L^3]^-$) moiety were explored.

Reaction of *N*-(pyridin-2-ylmethyl)-1,2-diaminoethane with 2,5-dihydroxybenzaldehyde and $Cu(ClO_4)_2\cdot 6H_2O$, $Cu(NO_3)_2\cdot 2.5H_2O$, CuCl or CuSCN in refluxing MeOH under N_2 affords green solutions, from which green or brown solids precipitate in moderate-to-high yields following cooling and concentration of the solutions. The solubilities of these products varied markedly depending on the anion used; however, all the complexes could be recrystallised from an appropriate solvent (see Experimental section). The recrystallised compounds analysed cleanly as $[CuL^2]X$ ($X^- = ClO_4^-$ **2**, NO_3^- **3**, Cl^- **4** or NCS^- **5**), a conclusion confirmed by FAB mass spectrometry which, for all compounds, exhibited an intense peak at $m/z = 332$, corresponding to $[Cu(L^2 - H)]^+$. The complex $[CuL^3]ClO_4$ **6** was also prepared, by an analogous template synthesis using $Cu(ClO_4)_2\cdot 6H_2O$ and 2,4,5-trihydroxybenzaldehyde; this product showed an intense peak from the fragment $[CuL^3]^+$ by FAB mass spectrometry, at $m/z = 349$. It is noteworthy that, in those reactions where copper(I) template salts were used, their oxidation to Cu^{II} proceeded cleanly during the template synthesis despite the anaerobic conditions used; the nature of the oxidising agent in these reactions is unclear.

Table 2 Selected bond lengths (Å) and angles (°) for $[CuL^2]ClO_4$ (**2**)

Cu(1)–N(2)	1.967(5)	Cu(1)–N(12)	1.915(5)
Cu(1)–N(9A)	2.010(7)	Cu(1)–O(20)	1.870(4)
Cu(1)–N(9B)	2.075(16)		
N(2)–Cu(1)–N(9A)	82.3(2)	N(9A)–Cu(1)–O(20)	166.0(3)
N(2)–Cu(1)–N(9B)	85.0(3)	N(9B)–Cu(1)–N(12)	82.5(3)
N(2)–Cu(1)–N(12)	167.5(2)	N(9B)–Cu(1)–O(20)	167.6(5)
N(2)–Cu(1)–O(20)	96.29(18)	N(12)–Cu(1)–O(20)	96.02(18)
N(9A)–Cu(1)–N(12)	86.2(2)		

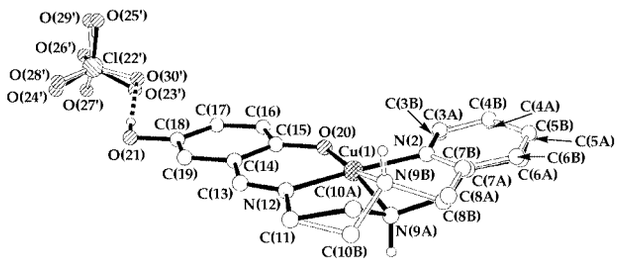

Fig. 5 View of the asymmetric unit in the structure of $[CuL^2]ClO_4$ **2**, showing the atom numbering scheme employed. Both the major (solid bonds) and minor (hollow bonds) disorder orientations for the cation and anion are shown. Primed atoms are related to unprimed atoms by the relation by $1 - x$, $-\frac{1}{2} + y$, $\frac{1}{2} - z$. For clarity, all C-bound H atoms have been omitted.

The IR spectroscopy of complex **5** as a Nujol mull shows an intense thiocyanate N–C stretch at 2043 cm^{-1}, consistent with an N-bound NCS^- ligand.[26] Presumably, this compound exists as a neutral square pyramidal $[Cu(NCS)(L^2)]$ complex, with an apical NCS^- ligand (*cf.* [CuCl(paip)][25]). For **2** and **6**, however, the single broad Cl–O vibration centred at 1070 cm^{-1} in the IR spectrum is consistent with a four-co-ordinate copper(II) complex containing a non-co-ordinated anion.[26] This suggestion was subsequently confirmed crystallographically (see below). It is unclear whether apical anion co-ordination occurs in the solid for **3** or **4**.

X-Ray quality crystals of $[CuL^2]ClO_4$ **2** were grown from MeCN–Et_2O. A view of the complex molecule is shown in Fig. 5, while selected metric parameters are given in Table 2. The structure is complicated by disorder of the $NC_5H_4CH_2NHC_2H_4$ portion of the ligand backbone in a 70 (C3A–C10A) : 30 (C3B–C10B) occupancy ratio (Fig. 5). The co-ordination geometries at copper in the two disorder orientations are indistinguishable, the Cu(1)–N(9A) and Cu(1)–N(9B) bond lengths, and the angles X–Cu(1)–N(9A) and X–Cu(1)–N(9B) [X = N(2), N(12) or O(20)], all being identical to within 3σ. The copper ion sits in a near-square planar environment, with unexceptional Cu–N and Cu–O distances and *trans* angles within the donor plane of 166.0(3)–167.6(5)°. In particular, the metric parameters at copper are essentially identical to those of the literature compound [CuCl(paip)], which exhibits a very long apical Cu ··· Cl distance.[25]

The ligand disorder in the structure is related to intermolecular hydrogen bonding of the ligand NH group in the crystal lattice (Fig. 6). In the major orientation, H(9A) forms a hydrogen bond to O(20′) of an adjacent molecule related by the operation $-x$, $-y$, $1 - z$, with N(9A) ··· O(20′) 3.106(9) Å and N(9A)–H(9A) ··· O(20′) 137°. There are also weaker hydrogen bonds to the major disorder orientation (see below) of a neighbouring anion also related by $-x$, $-y$, $1 - z$, with N(9A) ··· O(24′) 3.520(16) Å, N(9A)–H(9A) ··· O(24′) 140°. In the minor form, H(9B) is now hydrogen bonded to O(21″) related by x, $\frac{1}{2} - y$, $\frac{1}{2} + z$, with N(9B) ··· O(21″) 3.388(18) Å and N(9B)–H(9B) ··· O(21″) 135°. The increased number of hydrogen bonds in the former orientation is consistent with its being more populated in the crystal. The ClO_4^- anion is also disordered over two orientations which are best modelled with a 70 : 30 occupancy ratio. This suggests that the anion disorder

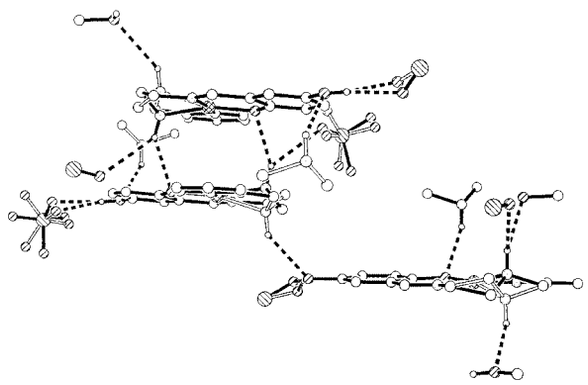

Fig. 6 Partial packing diagram of $[CuL^2]ClO_4$ **2**, showing the various intermolecular hydrogen bonding interactions in the lattice. Details as for Fig. 5. For clarity, the following simplifications have been made: only the major disorder orientation of atoms C(3)–C(8), *i.e.* C(3A)–C(8A), is shown; and, except for those interactions where the central molecule is the hydrogen-bond donor, only the donor/acceptor atom and those atoms immediately connected to it are given for each interaction.

may reflect the presence of two different cation conformations in the crystal. Three disordered O atoms of the anion are positioned to form hydrogen bonds to the 5-hydroxyl group of a neighbouring ligand related by $1 - x$, $-\frac{1}{2} + y$, $\frac{1}{2} - z$, with: O(23) ··· O(21‴) 2.918(14) Å, O(23) ··· H(21‴) ··· O(21‴) 175°; O(30) ··· O(28‴) 3.14(3) Å, O(30) ··· H(21‴) ··· O(21‴) 124°; and O(30) ··· O(21‴) 2.81(3) Å; O(30) ··· H(21‴) ··· O(21‴) 171°. There is also a hydrogen bond from O(24) to the amino moiety of a neighbouring cation in the major ligand disorder orientation (see above).

A dataset was also collected from weakly diffracting crystals of $[CuL^3]ClO_4$ [**6**; $a = 7.416(4)$, $b = 10.752(5)$, $c = 11.281(5)$ Å, $\alpha = 105.36(2)$, $\beta = 94.01(2)$, $\gamma = 99.52(2)°$, triclinic, space group $P\bar{1}$]. An initial refinement demonstrated that the co-ordination sphere at copper in this compound is indistinguishable from that of **2**, with a near-planar four-co-ordinate copper(II) centre and non-co-ordinated ClO_4^- anion. However, this structure also suffers from the ligand disorder described above which, given the inferior quality of the data, could not satisfactorily be resolved.

Since **3**–**5**, in particular, are only poorly soluble, to enable comparisons between these compounds all solution measurements on **2**–**6** were performed in dmf. Complexes **2**–**5** exhibit nearly identical UV/vis spectra at 298 K, showing a d–d band with $\lambda_{max} = 555 \pm 1$ nm ($\varepsilon_{max} = 190$–220 M^{-1} cm^{-1}) and O→Cu LMCT absorption at 410 nm (4100–4500 M^{-1} cm^{-1}). Similar peaks were observed for **6**, at $\lambda_{max} = 540$ (sh) and 388 nm (7100 M^{-1} cm^{-1}), respectively. All of the above complexes gave identical EPR spectra in dmf at 77 K, with $g_{\|} = 2.19$–2.20, $g_{\perp} = 2.05 \pm 0.01$, $A_{\|}\{^{63,65}Cu\} = 195 \pm 2$ G at 77 K. These spectra are typical of square planar $\{d_{x^2-y^2}\}^1$ or $\{d_{xy}\}^1$ copper(II) complexes,[21,23] while the ratio $g_{\|} : A_{\|}\{^{63,65}Cu, cm^{-1}\} = 110 \pm 1$ cm from these spectra is appropriate for a near-planar four-co-ordinate copper(II) centre.[27] We conclude that, in solution, **2** and **6** have identical co-ordination gometries at copper, and that, for **3**–**5**, substantial anion dissociation occurs in dmf to afford tetragonal $[Cu(L^2)(dmf)_x]^+$ ($x = 0$–2) as the dominant copper-containing species. As powdered solids, these complexes all exhibit isotropic signals at $\langle g \rangle = 2.07$–2.09.

Electrochemistry

Cyclic voltammograms of the ligands and complexes were run in dmf–0.1 M $NBu^n_4PF_6$ or MeCN–0.1 M $NBu^n_4PF_6$ at 293 K. Unless otherwise stated, all potentials quoted refer to measurements run at a scan rate ('v') of 100 mV s^{-1} and against an internal ferrocene–ferrocenium standard. The results of these experiments are summarised in Table 3. The nomenclature used to describe the voltammetric processes undergone by these

Table 3 Cyclic voltammetric data for the complexes in this study (dmf–0.1 M $NBu^n_4PF_6$ or MeCN–0.1 M $NBu^n_4PF_6$, 298 K, $v = 100$ mV s^{-1}). All potentials quoted *vs.* the ferrocene–ferrocenium couple. The nomenclature of ligand-centred processes corresponds to that we have previously employed in ref. 15

Compound	Solvent	P1 E_{pa}/V	P2 E_{pc}/V	P3 E_{pc}/V	C^{II}–Cu^{I} $E_{1/2}$/V (ΔE_p/mV)	Cu^{I}–Cu^{0} E_{pc}/V
HL^1	MeCN	+0.20	−0.42	−1.14[a]	—	—
1 $[\{Cu(\mu\text{-}L^1)\}_2](BF_4)_2$	MeCN	+0.44	−0.29	—	−0.56[b]	−1.03
2 $[CuL^2]ClO_4$	dmf	+0.30	—	−0.96	−1.34 (200)	—
	MeCN	+0.53	—	−0.72	−1.25[b]	—
3 $[CuL^2]NO_3$	dmf	+0.23	—	−0.99	−1.31 (240)	—
4 $[CuL^2]Cl$	dmf	+0.22	—	−0.93	−1.33 (220)	—
5 $[Cu(NCS)(L^2)]$	dmf	+0.22	—	−1.08	−1.39 (90)	—
6 $[CuL^3]ClO_4$	dmf	+0.10	—	−0.94	−1.36[b]	—

[a] Has an associated daughter oxidation, at $E_{pa} = +0.83$ V (corresponding to process P4 in ref. 15). [b] Irreversible process, E_{pc} value quoted (see text).

complexes follows our earlier electrochemical study of other hydroquinone-containing Schiff base complexes.[15]

The CV of HL^1 in MeCN shows a single irreversible oxidation ('P1') at $E_{pa} = +0.20$ V which exhibits two irreversible daughter processes: a weak irreversible peak ('P2') at $E_{pc} = -0.42$ V; and a stronger, broad quasi-reversible couple ('P3/P4') at $E_{1/2} = -0.99$ V ($\Delta E_p = 310$ mV). This pattern of daughter peaks, and their potentials, are all very similar to those we have previously reported for H_2L^4.[15] By analogy with this earlier study, we therefore assign P2 to the reduction of the protonated initial benzoquinonecarbaldimine product,[28] and the P3/P4 couple to the product of an electrochemical step–chemical step (EC) reaction resulting in decomposition of the benzoquinonecarbaldimine moiety. This decomposition reaction is probably catalysed by protons liberated during the initial oxidation.[15]

Complex **1** under the same conditions shows two irreversible ligand-based oxidation waves at $E_{pa} = +0.44$ and +0.81 V, with an approximately 1:2 intensity ratio that does not vary with scan rate. Two weak irreversible daughter peaks are associated with these oxidations, one of which can probably be assigned to the P2 process on the basis of its potential. This is different behaviour to that of $[CuL^4]$, which shows a single P1 oxidation and a similar pattern of P2–P4 daughter waves as observed for H_2L^4.[15] We tentatively assign these oxidations for **1** to oxidation of $[Cu(L^1)(MeCN)_x]^+$ and $[\{Cu(\mu\text{-}L^1)\}_2]^{2+}$, respectively, since the bridging hydroquinonate groups in the latter species would be expected to have a more positive oxidation potential. This is also consistent with the EPR spectrum of this compound in MeCN, which demonstrated the presence of a minor mononuclear solvolysis product (see above). In addition to these ligand-based peaks, two irreversible metal-based processes were detected for **1**: an irreversible Cu^{II}–Cu^{I} reduction at $E_{pc} = -0.56$ V (a shoulder on P1 near $E_{pa} = +0.25$ V was tentatively assigned to a Cu^{I}–Cu^{II} daughter reoxidation); and a Cu^{I}–Cu^{0} peak at $E_{pc} = -1.03$ V, with an associated copper-desorption spike near −0.6 V.

The voltammetric behaviour of complexes **2**–**6** in dmf is much closer to that exhibited by $[CuL^4]$.[15] The complexes exhibit two irreversible oxidations; a 2-electron P1 oxidation at $E_{pa} = 0.10$–0.30 V, and a weaker shoulder on the solvent front at $E_{pa} \approx 0.7$–0.8 V. There is one irreversible daughter reduction associated with the first oxidation, at a potential corresponding to P3 of $E_{pc} = -0.94$ to −1.08 V. Upon addition of the hindered base 2,6-dimethylpyridine to the samples, the P3 daughter product and (for **2**, **3** and **6**) second oxidation decrease significantly in intensity, while a P2 daughter oxidation appears at $E_{pc} = -0.4$ V. This behaviour is consistent with the same acid-catalysed ECE behaviour observed for HL^1, H_2L^4 and $[CuL^4]$.[15]

In addition to the above ligand-based processes, complexes **2**–**6** show a quasi-reversible one-electron reduction at $E_{\frac{1}{2}} = -1.31$ to −1.39 V, with $I_{pa}:I_{pc} \approx 0.7$, assignable to a Cu^{II}–Cu^{I} process. Although the forward peak in this process is almost invariant at $E_{pc} = -1.39$ to −1.44 V, the position and broadness of the return peak varies markedly depending on the anion present. This suggests that close association of the anions with the copper(I) centres may occur following reduction at the electrode surface. No Cu^{I}–Cu^{0} reduction was detected for **2**–**6**. Of all of **2**–**6**, only **2** was sufficiently soluble in MeCN to allow a cyclic voltammogram to be run. In this solvent, **2** shows an identical pattern of peaks as in dmf, showing that the ligand-based EC chemistry undergone by **2** is not solvent-dependent. The potentials of all these processes are slightly more positive in MeCN than their positions in dmf, however (Table 3).

Concluding remarks

Using a tetradentate N_3O Schiff base ligand system, we have succeeded in preparing tetragonal copper(II) complexes containing, in one case, a 2,4,5-trihydroxybenzene moiety. In principle, this latter compound (**6**) could be a good model to examine TOPA→Cu electron transfer in substrate-reduced CAO. However, the oxidative electrochemistry of the 2,5-dihydroxybenzaldimine and 2,4,5-trihydroxybenzaldimine substituents is complex, leading to decomposition of the resultant 1,4-benzoquinonecarbaldimine products. The products of these reactions have yet to be identified, which is something we are pursuing. In any case, the instability of our ligands to oxidation makes them extremely limited as CAO models, for which chemically reversible ligand-based redox is a prerequisite. In order to achieve this we are examining other ways to incorporate a 2,4,5-trihydroxyphenylate or hydroxybenzoquinonate moiety into a copper complex, aside from Schiff base condensation. We shall report these results in due course.

Experimental

Unless otherwise stated, all manipulations were carried out in air using commercial grade solvents. 2,5-Dihydroxybenzaldehyde (Aldrich), 2,4,5-trihydroxybenzaldehyde (Lancaster) and all copper salts (Avocado) were used as supplied, while *N*-(pyridin-2-ylmethyl)-1,2-diaminoethane was prepared by the literature procedure.[29]

Syntheses

2,5-Dihydroxy-*N*-{pyridin-2-ylmethyl}benzylideneamine (HL^1). To a solution of 2,5-dihydroxybenzaldehyde (3.5 g, 28.8×10^{-3} mol) in MeOH (150 cm^3) was added 2-(2-aminoethyl)pyridine (4.0 g, 28.8×10^{-3} mol). Following a 3 h reflux, the solvent was removed *in vacuo* to afford a yellow oil. Trituration with Et_2O afforded a yellow solid which was recrystallised from MeOH. Yield 5.7 g, 82% (Found: C, 69.2; H, 5.8; N, 11.6. Calc. for C_7H_7NO: C, 69.4; H, 5.8; N, 11.6%). mp 145–147 °C. EI mass spectrum: *m*/*z* 242, M^+; 123, $[C_6H_3\{OH\}_2CH_2]^+$ and 106, $[NC_5H_4C_2H_4]^+$. NMR spectra ($\{CD_3\}_2SO$, 298 K): ^1H, δ 12.50 (br, 1H, Ph OH^5), 8.98 (br, 1H, Ph OH^2), 8.51 (d, 4.8 Hz,

1H, py H^6), 8.41 (s, 1H, N=CH), 7.69 (dd, 7.7 and 7.4 Hz, 1H, py H^4), 7.28 (d, 7.7 Hz, 1H, py H^2), 7.22 (ddd, 7.4, 4.8 and 0.9 Hz, 1H, py H^5), 6.75 (m, 2H, Ph H^4 and H^6), 6.68 (d, 9.6 Hz, 1H, py H^3), 3.96 (t, 6.9 Hz, 2H, CH_2) and 3.08 (t, 6.9 Hz, 2H, CH_2). UV/vis (MeCN): λ_{max} = 208 nm (ε_{max} = 19 200 M^{-1} cm^{-1}), 231 (23 000) 256 (10 400), 345 (4200).

[{Cu(μ-L^1)}$_2$][BF$_4$]$_2$ 1. Reaction of HL^1 (0.30 g, 1.2×10^{-3} mol) and $Cu(BF_4)_2 \cdot xH_2O$ (0.39 g, 1.2×10^{-3} mol) in $MeNO_2$ (25 cm^3) at room temperature rapidly afforded a dark brown solution. This solution was filtered and concentrated to *ca.* 5 cm^3. Vapour diffusion of Et_2O afforded dark brown crystals. Yield 0.34 g, 69% (Found: C, 41.7; H, 3.4; N, 7.0. Calc. for $C_{28}H_{26}B_2Cu_2F_8N_4O_4.H_2O$: C, 42.0; H, 3.5; N, 7.0%). FAB mass spectrum: *m*/*z* 607, [$^{63}Cu_2(L^1)_2 - H]^+$ and 304, [$^{63}CuL^1]^+$. UV/vis (MeCN): λ_{max} = 207 nm (ε_{max} = 47100 M^{-1} cm^{-1}), 225 (36 800) 255 (19 100), 326 (8800), 390 (sh), 475 (sh), 610 (sh) and 900 (sh). IR spectrum (Nujol): 1633s, 1613m, 1283s, 1161m, 950–1150vs, 813s, 769m and 525m cm^{-1}.

[CuL^2]ClO$_4$ 2. A mixture of *N*-(pyridin-2-ylmethyl)-1,2-diaminoethane (0.15 g, 1.0×10^{-3} mol), 2,5-dihydroxybenzaldehyde (0.14 g, 1.0×10^{-3} mol) and $Cu(ClO_4)_2 \cdot 6H_2O$ (0.37 g, 1.0×10^{-3} mol) in MeOH (25 cm^3) was refluxed under N_2 for 3 h. The resultant yellow-green solution was then concentrated under vacuum, yielding a green-brown solid which was recrystallised from MeCN. Yield 0.19 g, 44% (Found: C, 41.4; H, 3.7; N, 9.5. Calc. for $C_{15}H_{16}ClCuN_3O_6$: C, 41.6; H, 3.7; N, 9.7%). FAB mass spectrum: *m*/*z* 432, [$^{63}Cu(L^2)^{35}ClO_4]^+$ and 332, [$^{63}Cu(L^2 - H)]^+$. UV/vis (dmf): λ_{max} = 410 nm (ε_{max} = 4500 M^{-1} cm^{-1}) and 556 (220). IR spectrum (Nujol): 3376m, 3265m, 1634s, 1610m, 1540s, 1301s, 1285s, 1229m, 950–1150vs, 846m, 815s, 767s, 722m, 659m, 625s, 575m and 417m cm^{-1}.

[Cu(NO$_3$)(L^2)] 3. Method as for complex **2**, using $Cu(NO_3)_2 \cdot H_2O$ (0.23 g, 1.0×10^{-3} mol). The product was a green-brown solid which could be recrystallised from MeCN. Yield 0.36 g, 91% (Found: C, 45.3; H, 4.0; N, 13.9. Calc. for $C_{15}H_{16}CuN_4O_5$: C, 45.5; H, 4.1; N, 14.1%). FAB mass spectrum: *m*/*z* 332, [$^{63}Cu(L^2 - H)]^+$. UV/vis (dmf): λ_{max} = 410 nm (ε_{max} = 4500 M^{-1} cm^{-1}) and 555 (220). IR spectrum (Nujol): 3239m, 3156m, 1639s, 1609m, 1538s, 1230s, 1148s, 1120m, 1092m, 1052m, 1034m, 1008m, 941m, 884m, 836m, 813s, 757s, 724m, 656m and 416m cm^{-1}.

[CuCl(L^2)] 4. Method as for complex **2**, using CuCl (0.10 g, 1.0×10^{-3} mol). The product was a green solid which could be recrystallised from MeOH. Yield 0.20 g, 54% (Found: C, 47.4; H, 4.5; N, 10.9. Calc. for $C_{15}H_{16}ClCuN_3O_2 \cdot \frac{1}{2}H_2O$: C, 47.6; H, 4.5; N, 11.1%). FAB mass spectrum: *m*/*z* 332, [$^{63}Cu(L^2 - H)]^+$. UV/vis (dmf): λ_{max} = 410 nm (ε_{max} = 4100 M^{-1} cm^{-1}) and 556 (190). IR spectrum (Nujol): 3190m, 1635s, 1608m, 1540s, 1302s, 1279s, 1227m, 1145s, 1098m, 1052m, 1033m, 1025m, 836m, 819s, 754s, 724m, 656m and 418m cm^{-1}.

[Cu(NCS)(L^2)] 5. Method as for complex **2**, using CuNCS (0.12 g, 1.0×10^{-3} mol). The product was a brown solid which was recrystallised from dmf–Et_2O–hexanes. Yield 0.30 g, 76% (Found: C, 48.9; H, 4.2; N, 14.2. Calc. for $C_{16}H_{16}CuN_4O_2S$: C, 49.0; H, 4.1; N, 14.3%). FAB mass spectrum: *m*/*z* 332, [$^{63}Cu(L^2 - H)]^+$. UV/vis (dmf): λ_{max} = 409 nm (ε_{max} = 4500 M^{-1} cm^{-1}) and 557 (220). IR spectrum (Nujol): 3240m, 2043s, 1634s, 1615m, 1557s, 1294s, 1280s, 1218s, 1116m, 1091m, 1047m, 1032m, 996m, 940s, 859m, 830m, 814s, 769s, 724m, 656m, 573m, 533m, 471m and 416m cm^{-1}.

[CuL^3]ClO$_4$ 6. A mixture of *N*-(pyridin-2-ylmethyl)-1,2-diaminoethane (0.15 g, 1.0×10^{-3} mol), 2,4,5-trihydroxybenzaldehyde (0.17 g, 1.0×10^{-3} mol) and $Cu(ClO_4)_2 \cdot 6H_2O$ (0.37 g, 1.0×10^{-3} mol) in MeOH (25 cm^3) was refluxed under N_2 for 3 h. The resultant yellow-green solution was then concentrated under vacuum and the green-brown solid isolated by filtration. The product was recrystallised from a 1:1 MeCN:MeOH mixture. Yield 0.42 g, 93% (Found: C, 40.0; H, 3.5; N, 9.1. Calc. for $C_{15}H_{16}ClCuN_3O_7$: C, 40.1; H, 3.6; N, 9.3%). FAB mass spectrum: *m*/*z* 349, [$^{63}CuL^3]^+$. UV/vis (dmf): λ_{max} = 388 nm (ε_{max} = 7100 M^{-1} cm^{-1}) and 540 (sh). IR spectrum (Nujol): 3373s, 3242s, 1631s, 1611m, 1552s, 1513s, 1434s, 1343m, 1282s, 1250s, 950–1150vs, 876s, 786s, 763s, 721m, 658m, 621s, 600m and 406m cm^{-1}.

Table 4 Experimental details for the single crystal structure determinations

	[{Cu(μ-L^1)}$_2$][BF$_4$]$_2$·MeNO$_2$ **1**·MeNO$_2$	[CuL^2]ClO$_4$ **2**
Formula	$C_{29}H_{29}B_2Cu_2F_8N_5O_6$	$C_{15}H_{16}ClCuN_3O_6$
M_r	844.27	433.30
Crystal class	Triclinic	Monoclinic
Space group	$P\bar{1}$	$P2_1/c$
a/Å	14.605(4)	7.683(1)
b/Å	12.551(3)	11.404(1)
c/Å	11.021(3)	19.242(1)
α/°	106.74(2)	—
β/°	75.19(3)	99.56(1)
γ/°	71.34(2)	—
V/Å^3	1692.9(8)	1662.5(3)
Z	2	4
μ(Mo-Kα)/mm^{-1}	1.350	1.514
T/K	150(2)	180(2)
Measured reflections	4617	11232
Independent reflections	4407	2891
R_{int}	0.050	0.076
R(*F*)	0.067	0.064
wR(*F*^{2})	0.183	0.145

Single crystal structure determinations

Crystals of complexes **1**·$MeNO_2$ and **2** were grown by vapour diffusion of Et_2O into solutions of the complexes in $MeNO_2$ and MeCN, respectively. Experimental details from the structure determinations are given in Table 4. All structures were solved by direct methods (SHELXTL Plus [30]) and refined by full matrix least squares on F^2 (SHELXL 93 [31] or 97 [32]).

[{Cu(μ-L^1)}$_2$][BF$_4$]$_2$·MeNO$_2$ (1·MeNO$_2$). During refinement the BF_4^- anion that does not interact with the Cu was found to be disordered by rotation about one B–F bond. This disorder was modelled over 3 orientations with a 0.5:0.3:0.2 occupancy ratio, using B–F and F···F distances restrained to values of 1.36(2) and 2.22(2) Å. All fully occupied non-H atoms were refined anisotropically, and all H atoms were placed in calculated positions.

[CuL^2]ClO$_4$ 2. Following an initial refinement using an ordered chelate ligand, abnormally high thermal parameters at atoms in the $NC_5H_4C_2H_4NHCH_2$ portion of the ligand were indicative of disorder. The atoms C(3)–C(10) were therefore modelled over two orientations: C(3A)–C(10A) with an occupancy of 0.7; and C(3B)–C(10B) with an occupancy of 0.3. All equivalent bond lengths within the two orientations were restrained to be equal with an esd of 0.02 Å, and equivalent 1,3-interatomic distances were restrained to be equal with an esd of 0.01 Å. Disorder of the O atoms of the ClO_4^- anion was modelled using 2 orientations O(23)–O(26) and O(27)–O(30) with a 0.7:0.3 occupancy ratio, using Cl–O and O···O distances restrained to be the same value with an esd of 0.03 Å. All non-H atoms with occupancies > 0.5 were refined anisotropically, and all H atoms were placed in calculated positions.

CCDC reference number 186/1916.

See http://www.rsc.org/suppdata/dt/b0/b001320j/ for crystallographic files in .cif format.

Other measurements

Infrared spectra were obtained as Nujol mulls pressed between KBr windows, between 400 and 4000 cm^{-1} using a Perkin-Elmer Paragon 1000 spectrophotometer, UV/visible spectra with a Perkin-Elmer Lambda 12 spectrophotometer operating between 200 and 1100 nm, in 1 cm quartz cells, NMR spectra on a Bruker DPX250 spectrometer operating at 250.1 (^1H) and 62.9 MHz (^{13}C) and mass spectra on a Kratos MS890 spectrometer, the fast atom bombardment spectra employing a 3-nitrobenzyl alcohol matrix. CHN microanalyses were performed by the University of Cambridge Department of Chemistry microanalytical service. X-Band EPR spectra were obtained using a Bruker ER200D spectrometer. Melting points are uncorrected. Variable temperature magnetic susceptibility measurements were obtained using a Quantum Design SQUID magnetometer operating at 1000 G. A diamagnetic correction for the sample was estimated from Pascal's constants;[19] a diamagnetic correction for the sample holder was also applied. Observed and calculated data were refined using SIGMAPLOT.[33]

All electrochemical measurements were carried out using an Autolab PGSTAT20 voltammetric analyser, in dmf or MeCN containing 0.1 M $NBu^n_4PF_6$ as supporting electrolyte. Cyclic voltammetric experiments involved the use of a double platinum working/counter electrode and a silver wire reference electrode; all potentials quoted are referenced to an internal ferrocene–ferrocenium standard and were obtained at a scan rate of 100 mV s^{-1}. The number of electrons involved in a given voltammetric process was determined by comparison of the peak height with that of the Fe^{II}–Fe^{III} couple shown by an equimolar amount of ferrocene.

Acknowledgements

The authors gratefully acknowledge funding by The Royal Society (M. A. H.), the EPSRC and I.C.I. R&T Division (N. K. S.), the Committee of Vice Chancellors and Principles (P. L.), the European Union (Marie Curie Fellowship to H. E.), the University of Cambridge and the University of Leeds.

References

1 J. P. Klinman and D. Mu, *Annu. Rev. Biochem.*, 1994, **63**, 299; J. P. Klinman, *Chem. Rev.*, 1996, **96**, 2541; C. Anthony, *Biochem. J.*, 1996, **320**, 697.
2 R. A. Scott and D. M. Dooley, *J. Am. Chem. Soc.*, 1985, **107**, 4348; P. F. Knowles, R. W. Strange, N. J. Blackburn and S. S. Hasnain, *J. Am. Chem. Soc.*, 1989, **111**, 102.
3 G. J. Baker, P. F. Knowles, K. B. Pandeya and J. B. Rayner, *Biochem. J.*, 1986, **237**, 609; J. McCracken, J. Peisach and D. M. Dooley, *J. Am. Chem. Soc.*, 1987, **109**, 4064.
4 T. J. Williams and M. C. Falk, *J. Biol. Chem.*, 1986, **261**, 15949; D. M. Dooley, M. A. McGuirl, C. E. Cote, P. F. Knowles, I. Singh, M. Spiller, R. D. Brown III and S. H. Koenig, *J. Am. Chem. Soc.*, 1991, **113**, 754.
5 D. Mu, K. F. Medzihradsky, G. W. Adams, P. Mayer, W. M. Hines, A. L. Burlingame, A. J. Smith, D. Cai and J. P. Klinman, *J. Biol. Chem.*, 1994, **269**, 9926.
6 M. R. Parsons, M. A. Convery, C. M. Wilmot, K. D. S. Yadav, V. Blakeley, A. S. Corner, S. E. V. Phillips, M. J. McPherson and P. F. Knowles, *Structure*, 1995, **3**, 1171; V. Kumar, D. M. Dooley, H. C. Freeman, J. M. Guss, I. Harvey, M. A. McGuirl, M. J. C. Wilce and V. M. Zubak, *Structure*, 1996, **4**, 943; M. C. J. Wilce, D. M. Dooley, H. C. Freeman, J. M. Guss, H. Matsunami, W. S. McIntire, C. E. Ruggiero, K. Tanizawa and H. Yamaguchi, *Biochemistry*, 1997, **36**, 16116; R. Li, J. P. Klinman and F. S. Mathews, *Structure*, 1998, **6**, 293.
7 S. M. Janes, D. Mu, D. Wemmer, A. J. Smith, S. Kaur, D. Maltby, A. L. Burlingame and J. P. Klinman, *Science*, 1990, **248**, 981.
8 F. Wang, J.-Y. Bae, A. R. Jacobson, Y. Lee and L. M. Sayre, *J. Org. Chem.*, 1994, **59**, 2409; Y. Lee and L. M. Sayre, *J. Am. Chem. Soc.*, 1995, **117**, 3096, 11823; M. Murae and J. P. Klinman, *J. Am. Chem. Soc.*, 1993, **115**, 7117; *J. Am. Chem. Soc.*, 1995, **117**, 8698; *J. Am. Chem. Soc.*, 1995, **117**, 8707.
9 Q. Su and J. P. Klinman, *Biochemistry*, 1998, **37**, 12513.
10 C. M. Wilmot, J. Hadju, M. J. McPherson, P. F. Knowles and S. E. V. Phillips, *Science*, 1999, **286**, 1724.
11 D. M. Dooley, W. S. McIntire, M. A. McGuirl, C. E. Cote and J. L. Bates, *J. Am. Chem. Soc.*, 1990, **112**, 2782; D. M. Dooley, M. A. McGuirl, D. E. Brown, P. N. Turowski, W. S. McIntire and P. F. Knowles, *Nature* (*London*), 1991, **349**, 262; P. N. Turowski, M. A. McGuirl and D. M. Dooley, *J. Biol. Chem.*, 1993, **268**, 17680; D. M. Dooley and D. E. Brown, *J. Biol. Inorg. Chem.*, 1996, **1**, 205.
12 N. Nakamura, T. Kohzuma, H. Kuma and S. Suzuki, *J. Am. Chem. Soc.*, 1992, **114**, 6550; S. Suzuki, K. Yamaguchi, N. Nakamura, Y. Tagawa, H. Kuma and T. Kawamoto, *Inorg. Chim. Acta*, 1998, **283**, 260.
13 J. Rall, M. Wanner, M. Albrecht, F. M. Hornung and W. Kaim, *Chem. Eur. J.*, 1999, **5**, 2802.
14 E. Waldhör, B. Schwederski and W. Kaim, *J. Chem. Soc.*, *Perkin Trans. 2*, 1993, 2109.
15 E. H. Charles, L. M. L. Chia, J. Rothery, E. L. Watson, E. J. L. McInnes, R. D. Farley, A. J. Bridgeman, F. E. Mabbs, C. C. Rowlands and M. A. Halcrow, *J. Chem. Soc.*, *Dalton Trans.*, 1999, 2087.
16 M. A. Halcrow, L. M. L. Chia, X. Liu, E. J. L. McInnes, L. J. Yellowlees, F. E. Mabbs and J. E. Davies, *Chem. Commun.*, 1998, 2465; M. A. Halcrow, L. M. L. Chia, X. Liu, E. J. L. McInnes, L. J. Yellowlees, F. E. Mabbs, I. J. Scowen, M. McPartlin and J. E. Davies, *J. Chem. Soc.*, *Dalton Trans.*, 1999, 1753.
17 A. G. Orpen, L. Brammer, F. H. Allen, O. Kennard, D. G. Watson and R. Taylor, *J. Chem. Soc.*, *Dalton Trans.*, 1989, S1.
18 L. K. Thompson, S. K. Mandal, S. S. Tandon, J. N. Bridson and M. K. Park, *Inorg. Chem.*, 1996, **35**, 3117.
19 C. J. O'Connor, *Prog. Inorg. Chem.*, 1982, **29**, 203.
20 M. F. Charlot, S. Jeannin, Y. Jeannin, O. Kahn, J. Lucrece-Abaul and J. Martin-Frere, *Inorg. Chem.*, 1979, **18**, 1675.
21 B. A. Goodman and J. B. Raynor, *Adv. Inorg. Chem.*, 1970, **13**, 135.
22 E. I. Solomon, K. W. Penfield and D. E. Wilcox, *Struct. Bonding* (*Berlin*), 1983, **53**, 1.
23 A. B. P. Lever, *Inorganic Electronic Spectroscopy*, 2nd edn., Elsevier, Amsterdam, 1984, pp. 554–572.
24 Y. Maeda, K. Kawano and T. Oniki, *J. Chem. Soc.*, *Dalton Trans.*, 1995, 3533.
25 H. Luo, P. E. Fanwick and M. A. Green, *Inorg. Chem.*, 1998, **37**, 1127.
26 K. Nakamoto, *Infrared and Raman Spectra of Inorganic and Coordination Compounds, Part B*, 5th edn, J. Wiley and Sons, New York, 1997, Section III.
27 J. Gouteron, S. Jeannin, Y. Jeannin, J. Livage and C. Sanchez, *Inorg. Chem.*, 1984, **23**, 3387.
28 J. Q. Chambers, *The Chemistry of the Quinoid Compounds*, ed. S. Patai, Wiley, New York, 1974, ch. 14, pp. 737–791; *The Chemistry of the Quinoid Compounds*, *vol. 2*, eds. S. Patai and Z. Rappoport, Wiley, New York, 1988, ch. 12, pp. 719–757.
29 G. A. Gettys and C. D. Gutsche, *Bioorg. Chem.*, 1978, **7**, 141.
30 G. M. Sheldrick, SHELXTL Plus, PC version, Siemens Analytical Instruments Inc., Madison WI, 1990.
31 G. M. Sheldrick, SHELXL 93, University of Göttingen, 1993.
32 G. M. Sheldrick, SHELXL 97, University of Göttingen, 1997.
33 SIGMAPLOT, Program for Tabulating, Modelling and Displaying Data (v. 5.0), SPSS Inc., Chicago, IL, 1999.